

# Cascabela thevetia plant extract as corrosion inhibitor for carbon steel in polluted sodium chloride solution

## Abstract

The inhibiting effect of Cascabela Thevetia extract (CTE) in polluted sodium chloride (3.5% NaCl+16 ppmNa<sub>2</sub>S) on the corrosion of carbon steel (CS) was studied by weight loss (WL), potentiodynamic polarization (PP), electrochemical frequency modulation (EFM) and electrochemical impedance spectroscopy (EIS) techniques. The results showed that the inhibition efficiency (IE) increases with increase in extract dose and decreases with raising the temperature. %IE reached to ~95% at 300 ppm CTE. The obtained results indicated that the investigated extract is physically adsorbed on the CS surface and follows Freundlich adsorption isotherm. The PP data revealed that this extract acts as mixed type inhibitor. Surface morphology was tested using atomic force microscope (AFM) technique. Some quantum chemical calculations were used to support the experimental data. The results obtained from the different techniques are in good agreement.

**Keywords:** corrosion inhibition, carbon steel, polluted nacl, cascabela thevetia extract, adsorption

Volume 6 Issue I - 2017

**Fouda AS, Emam A, Refat R, Nageeb M**

Department of Chemistry, Faculty of Science, El-Mansoura University, Egypt

**Correspondence:** Fouda AS, Department of Chemistry, Faculty of Science, El-Mansoura University, El-Mansoura- 35516, Egypt, Tel +2 050 2365730, Fax +2 050 2202271, Email asfouda@hotmail.com

**Received:** August 26, 2017 | **Published:** September 18, 2017

**Abbreviations:** CTE, cascabela thevetia extract; CS, carbon steel; WL, weight loss; PP, potentiodynamic polarization; EFM, electrochemical frequency modulation; EIS, electrochemical impedance spectroscopy; IE, inhibition efficiency; AFM, atomic force microscope; SCE, saturated calomel electrode; OCP, open circuit potential

## Introduction

Corrosion of materials causes big losses in the economy of many countries due to the huge amount of funds needed to reduce it. Corrosion inhibition of metals, especially of CS, has received some attention because of its excellent mechanical properties, low cost and widespread use in the industry such as chemical processing, petroleum production, refining, transportation, pipelines, mining, construction industry, marine applications, thus, researches in the field of corrosion inhibition of steel is necessary. Seawater contains the remains of dead organisms, coral reefs, ships and boats which all are rot and lead to escalation of gases such as H<sub>2</sub>S and Na<sub>2</sub>S and other gases react with chlorine and hydrogen produce polluted NaCl. Among the several methods of corrosion control is the use of inhibitors. The studies of plant extracts as corrosion inhibitors are of great interest from an environmental perspective and are attracting a significant level of attention.<sup>1-3</sup> The safety and environmental issues of corrosion inhibitors arisen in industries has always been a global concern. Green inhibitors which have a promising future for the quality of the environment because they do not contain toxic compounds or heavy metals as Pb or Fe, so in the marine environment we should use natural plant inhibitors to overcome the corrosion problem and to protect the marine environment at the same time. So receive attention for the replacement of synthesized inorganic inhibitors which are often toxic, expensive, carcinogenic and environmentally unfriendly.<sup>4</sup> Plant extract is low cost and environmental safe, so the main advantages of using plant extracts as corrosion inhibitors are economic and safe environment. Several studies have been carried out on the protection of corrosion of metals and alloys by plant extracts such as: coffee ground,<sup>5</sup> Ruta Graveolens,<sup>6</sup> Murraya Koenigii,<sup>7</sup> Watermelons Rind,<sup>8</sup>

Oxandra Asbeckii,<sup>9</sup> Euphorbia Falcata,<sup>10</sup> Osmanthus Fragan Leaves,<sup>11</sup> Punica Plant,<sup>12</sup> Henna,<sup>13</sup> Tita Cordata,<sup>14</sup> Curcum plant<sup>15</sup> Delonix Regia leaf.<sup>16</sup> Nonetheless, there is still a need for research on other plants can be used as inhibitors in industrial applications.

This present study seeks to:

- Investigate the effectiveness of thoroughly Cascabela Thevetia extract in inhibiting the corrosion of CS immersed in polluted NaCl solution.
- Develop a model that can predict the experimental corrosion rate-resulting from the inhibition.
- Figure out the adsorption isotherm that the extract obeys in polluted NaCl medium.

## Experimental methods

### Materials and solutions

Tests were performed on rectangular specimens with dimensions 2x2x0.1cm of CS with the following chemical composition in weight %: C 0.200, Mn 0.350, P 0.024, Si 0.003 and Fe balance. CS samples (2x2x0.2cm) mechanically abraded with different grades (22-1200) of sand paper and polished by 0.25 micron alumina powder to approach the mirror surface, then degreased, hand washed with bidistilled water and rinsed with ethanol, finally used in weight loss tests.

### Solution preparation

The polluted sodium chloride (3.5%NaCl+16ppmNa<sub>2</sub>S) solution was prepared from NaCl and Na<sub>2</sub>S (Merck) and bi-distilled water. The concentration range of Cascabela Thevetia extract varied from 50 to 300ppm and the electrolyte used was 100 ml for each experiment.

### Stock solution of cascabela thevetia extract

Stock solution of the Cascabela Thevetia extract was prepared by boiling 20-25g of air-dried Cascabela Thevetia adult leaves in bidistilled water and left overnight. The Cascabela Thevetia leaves

were air-dried earlier in natural sunlight until the final mass became constant. The contents of the extraction process were then mixed in a plinder, filtered and the resulting solution was kept in a refrigerator at low temperatures of 2-3oC in order to prevent the contents of the extract from being altered due to the chemical, physical, and biological reactions it might otherwise undergo.<sup>17</sup>

### Weight loss measurements

The weighted samples they immersed in 100ml of polluted NaCl with and without different doses of CTE. The immersion time of the weight loss test is 30, 60, 90, 120, 150 and 180min the CS samples were taken out, washed with bidistilled water, dried and weighted again. The results of the weight loss tests are the mean of three runs, each with fresh specimen and 100 ml of fresh polluted NaCl solution. The inhibition efficiency (%IE) and the degree of surface coverage ( $\theta$ ) were calculated using the following equation:

$$\%IE = \theta \times 100 = \left[ (W^o - W) / W^o \right] \times 100 \quad (1)$$

Where  $W_o$  and  $W$  are the values of the average weight losses in the absence and presence of the extract, respectively.

### Polarization measurements

Polarization experiments were carried out in a conventional three-electrode cell with platinum gauze as the auxiliary electrode and a saturated calomel electrode (SCE) coupled to a fine Luggin capillary as reference electrode. The working electrode was in the form of a square cut from CS sheet of equal composition embedded in epoxy resin of poly tetrafluoroethylene so that the flat surface area was 1 cm<sup>2</sup>. Prior to each measurement, the electrode surface was pretreated in the same manner as the weight loss experiments. Before measurements, the electrode was immersed in solution for 30 min. until a steady state was reached. The potential was started from -600 to +400mV vs open circuit potential (OCP) with a scan rate 1 mVs-1. All experiments were performed at 25oC and the results were always repeated at least three times to check the reproducibility. The %IE and  $\theta$  were calculated using the following equation:

$$\%IE = \theta \times 100 = \left[ 1 - (i_{corr} / i_{corr}^o) \right] \times 100 \quad (2)$$

Where,  $i_{corr}^o$  and  $i_{corr}$  are corrosion current densities of CS in the absence and presence of extract, respectively.

### Electrochemical impedance spectroscopy (EIS)

Impedance measurements were carried out in the frequency range of 100 kHz to 0.1 Hz and peak to peak ac amplitude of 5 mV. All impedance data were fitted to appropriate equivalent circuit using the Gamry Echem Analyst software version 6.03. The %IE and  $\theta$  were calculated using the following equation:

$$\%IE_{EIS} = \left[ 1 - (R_{ct}^o / R_{ct}) \right] \times 100 \quad (3)$$

Where,  $R_{ct}^o$  and  $R_{ct}$  are the charge-transfer resistance values without and with inhibitor respectively. The double layer capacity was calculated using the following equation:

$$C_{dl} = 1 / (R_{ct} 2\pi f_{max}) \quad (4)$$

Where  $f_{max}$  is the frequency maximum

### Electrochemical frequency modulation (EFM)

EFM experiments were performed with applying potential perturbation signal with amplitude 10 mV with two sine waves of 2 and 5 Hz. The choice for the frequencies of 2 and 5Hz was based

on three arguments.<sup>18</sup> The larger peaks were used to calculate the corrosion current density ( $i_{corr}$ ), the Tafel slopes ( $\beta_c$  and  $\beta_a$ ) and the causality factors CF-2 and CF-<sup>19</sup>.

All electrochemical experiments were carried out using Gamry instrument PCI300/4 Potentiostat/Galvanostat/Zra analyzer, DC105 corrosion software, EIS300 electrochemical impedance spectroscopy software, EFM140electrochemical frequency modulation software and Echem Analyst 5.5 for results plotting, graphing, data fitting and calculating.

### Surface analysis

For morphological study, surface features (1x1x0.1cm) of CS were examined before and after exposure to polluted NaCl solutions for 24 hours with and without the CTE.

## Results and discussion

### Weight Loss (WL) Measurements

WL of CS was determined, at various time intervals without and with different doses of CTE. The obtained WL- time curves are represented in Figure 1 for CTE. The IE of this extract was found to be dependent on the extract dose. The curves obtained in the presence of the extract fall significantly below that of its absence. The increase in the extract dose was accompanied by a decrease in WL, an increase of  $\theta$  and an increase in the %IE. These results lead to the conclusion that this extract is fairly efficient as inhibitor for CS dissolution in polluted NaCl solution. The data obtained are summarized in Table 1.

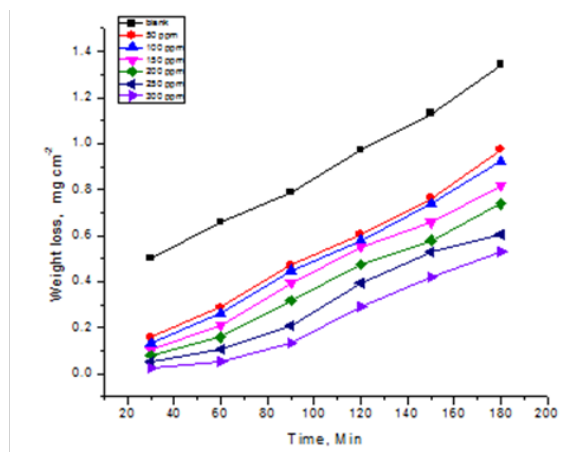


**Figure 1** WL-time curves for the corrosion of CS in polluted NaCl without and with different doses of Cascabela Thevetia extract at 25°C.

### Effect of temperature

The effect of temperature on the CR of CS in polluted NaCl in presence of different doses of the extract was studied in the temperature range of 25-45oC using WL measurements. As indicated from Table 2, the rate of CS dissolution increases as the temperature increases, but at lower rate than in uninhibited solutions, this indicated that the raising of temperature led to the reduction of the extract adsorption and then the acceleration of dissolution process,<sup>20</sup> which proves that the adsorption of the extract on the surface of CS occurs through physical adsorption.

### Adsorption isotherms

One of the most convenient ways of expressing adsorption quantitatively is by deriving the adsorption isotherm that characterizes

the metal/inhibitor/ environment system. The basic information on the interaction between the inhibitor and the metal surface can be provided by the adsorption isotherm, and the type of the inhibitors on metal is influenced by:

- The nature and charge of the metal.
- Chemical structure of the inhibitor and
- The type of electrolyte.

The values of the ( $\theta$ ) were evaluated at different doses of the extract in polluted NaCl solution. Various adsorption isotherms were applied to fit  $\theta$  values, but the best fit was found to obey Freundlich adsorption isotherm which is represented in Figure 2 for Cascabela Thevetia at 25°C, Freundlich adsorption isotherm expressed by Eq. 5:

$$\theta = K_{ads} C^n \quad (5)$$

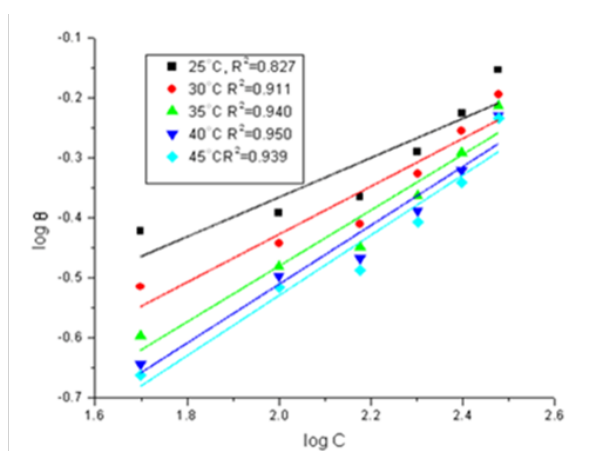


**Figure 2** Freundlich adsorption isotherm for Cascabela Thevetia extract on CS surface in polluted NaCl at different temperatures.

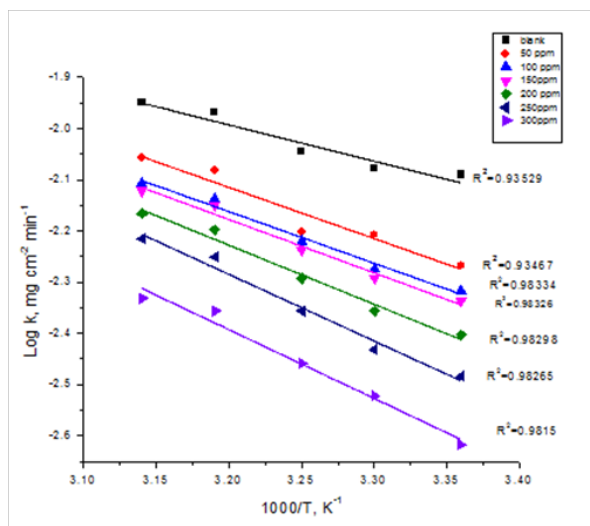


**Figure 3** Log  $k_{corr}$  vs.  $1/T$  curves for CS corrosion after 120 minutes of immersion in polluted NaCl with and without various doses of CTE.

Where,  $C$  is the dose (ppm) of the extract in the bulk electrolyte, and  $K_{ads}$  is the adsorption equilibrium constant. A plot of  $\theta$  versus  $C$  should give straight lines with slope equals to  $2.303/a$  and intercept ( $2.303/a \log K_{ads}$ ). The experimental data give good curves fitting for the applied adsorption isotherm as the correlation coefficients ( $R^2$ ) were in the range (0.978-0.919).  $K_{ads}$  obtained from the intercepts

of Freundlich adsorption isotherm and is related to free energy of adsorption  $\Delta G_{ads}^0$  as follows:

$$K_{ads} = 1 / 55.5 \exp(-\Delta G_{ads}^0 / RT) \quad (6)$$

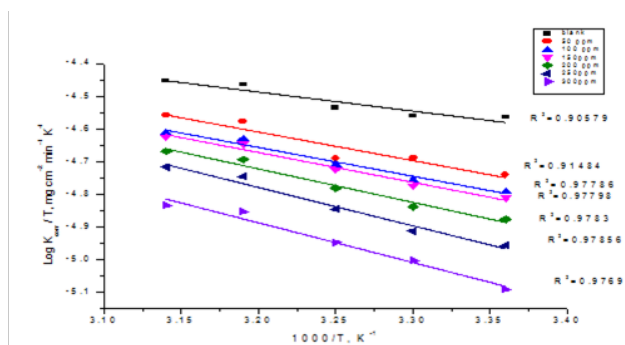


**Figure 4** Log ( $k_{corr}/T$ ) vs  $1/T$  curves for transition plots for CS corrosion rates ( $k_{corr}$ ) after 120 minutes of immersion in polluted NaCl with and without various doses of CTE.

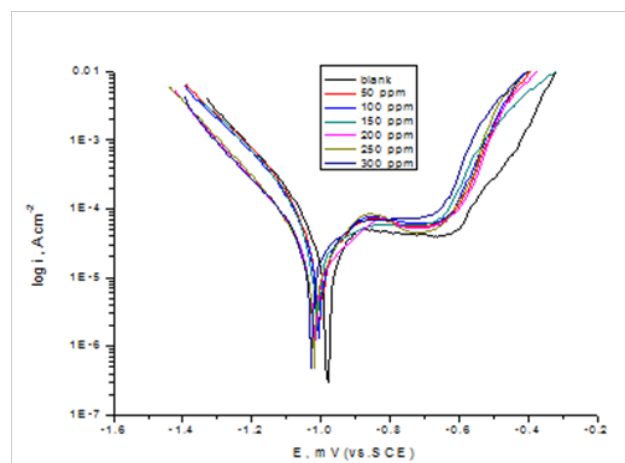


**Figure 5** PP curves for the dissolution of CS in polluted NaCl with and without different doses of CTE at 25oC.

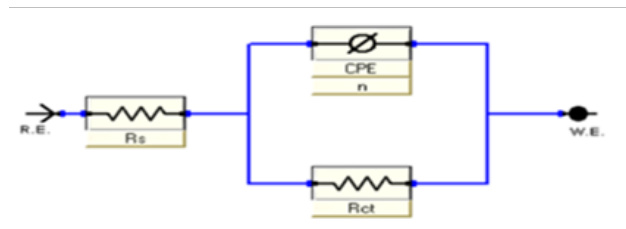


**Figure 6** Equivalent circuit model used to fit experimental EIS.

Where,  $R$  is the universal gas constant,  $T$  is the absolute temperature and 55.5 is molar dose of water in the solution.

The value of  $K_{ads}$  and  $\Delta G_{ads}^0$  for the plant extract were calculated and are recorded in Table 3. The negative value of  $\Delta G_{ads}^0$  ensures the spontaneity of the adsorption process and stability of the adsorbed layer on the steel surface. Generally, values of  $\Delta G_{ads}^0$  around -20 kJ mol<sup>-1</sup> or lower are consistent with the electrostatic interaction between the charged molecules and the charged metal (physisorption). The values of  $K_{ads}$  were found to run parallel to the %IE. The heat of adsorption ( $\Delta H_{ads}^0$ ) and the change in entropy ( $\Delta S_{ads}^0$ ) can be calculated according to the thermodynamic basic Eq.7.

$$\Delta G_{ads}^0 = \Delta H_{ads}^0 - T \Delta S_{ads}^0 \quad (7)$$

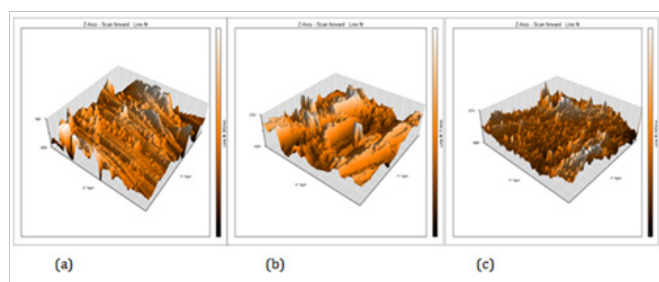


**Figure 7** AFM micrograph of CS surface (a) before immersion in polluted NaCl, (b) after 24h immersion in polluted NaCl, (c) after 24h immersion in polluted NaCl + 300 ppm of CTE.

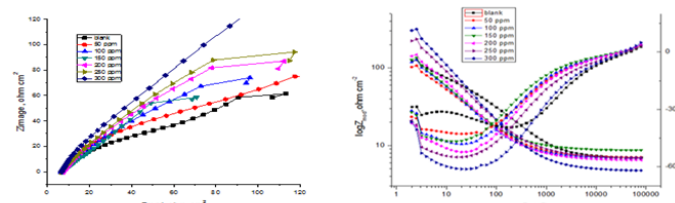


**Figure 8** Nyquist (a) and Bode (b) plots for the corrosion of CS in polluted NaCl with and without different doses of CTE at 25°C.

The absolute values of  $\Delta H^{\circ}_{\text{ads}}$  obtained in this study was lower than ( $40 \text{ kJ mol}^{-1}$ ), this indicative of physisorption.<sup>21</sup> In the present case, the negative values of  $\Delta H^{\circ}_{\text{ads}}$  indicate that this extract may be adsorbed physically and chemically on CS surface. The  $\Delta S^{\circ}_{\text{ads}}$  values in the presence of extract in polluted NaCl are negative. This indicates that decrease in disorder takes places on going from reactants to the metal-adsorbed reaction complex.<sup>22</sup>

### Kinetic –thermodynamic corrosion parameter

The activation parameters for the corrosion process were calculated from Arrhenius-type plot according to Eq.8:

$$k_{\text{corr}} = A \exp(-E_a^* / RT) \quad (8)$$

Where,  $E_a^*$  is the apparent activation energy, R is the universal gas constant and A is the Arrhenius pre-exponential constant. Values of apparent activation energy of corrosion for CS in polluted NaCl without and with various doses of CTE are shown in Table 4. These values were determined from the slope of  $\log(k_{\text{corr}})$  versus  $1/T$  plots are shown in Figure 3. The results of Table 5 showed that the value of ( $E_a^*$ ) for inhibited solution is higher than that for uninhibited solution, suggesting that dissolution of CS is slow in the presence of the extract. It is known from Arrhenius equation that the higher ( $E_a^*$ ) values lead to the lower corrosion rate, this is due to the formation of a film on the CS surface serving as an energy barrier for the CS corrosion.<sup>23</sup> Schmidt et al.<sup>24</sup> found that organic molecules inhibit both the anodic and cathodic partial reactions on the electrode surface and a parallel reaction takes place on the covered area but the reaction rate on the covered area is substantially less than on the uncovered area similar to the present study. The alternative formulation of transition state equation is shown in Eq. 9:

$$k_{\text{corr}} = RT / Nh \exp(\Delta S^* / R) \exp(-\Delta H^* / RT) \quad (9)$$

Where,  $k_{\text{corr}}$  is the rate of metal dissolution, h is Planck's constant; N is Avogadro's number, is the entropy of activation and is the enthalpy of activation. Figure 4 shows a plot of ( $\log k_{\text{corr}}/T$ ) against ( $1/T$ ) in the case of Cascabela Thevetia in polluted NaCl. Straight

lines are obtained with a slopes equal to ( $\Delta H^* / 2.303R$ ) and intercepts are [ $\log(R/Nh + \Delta S^* / 2.303R)$ ]. These results are presented in Table 4.

The positive signs of the enthalpies ( $\Delta H^*$ ) reflect the endothermic nature of the CS dissolution process. The entropy of activation in presence and absence of the extract was large and negative. This implies that the activated complex in the rate determining step represents association rather than dissociation, indicating that a decrease in disorder takes place, going from reactant to the activated complex.<sup>25</sup>

### Potentiodynamic Polarization (PP) Measurements

Figure 5 shows the PP curves of CS dissolution in polluted NaCl in the absence and presence of different doses of Cascabela Thevetia extract at 25°C. The numerical values of the variation of the corrosion current density ( $i_{\text{corr}}$ ), the corrosion potential ( $E_{\text{corr}}$ ), Tafel slopes ( $\beta_a$  and  $\beta_c$ ), the ( $\theta$ ) and %IE were recorded in Table 5. The IE and  $\theta$  were calculated using Eq.2

The results of Table 5 indicate that:

- The cathodic and anodic curves obtained exhibit Tafel-type behavior. Addition of CTE increases both the cathodic and anodic overvoltage and inhibits both the hydrogen evolution and the anodic dissolution processes i.e. mixed type inhibitor.
- The corrosion current density ( $i_{\text{corr}}$ ) decreases with increasing the dose of the Cascabela Thevetia which indicates that the extract acts as inhibitor, and the degree of inhibition depends on the dose and type of extract present.
- The slopes of anodic and cathodic Tafel lines ( $\beta_a$  and  $\beta_c$ ), were slightly changed on increasing the dose of the tested extract. This indicates that this extract acts as mixed-type inhibitor. Tafel lines are parallel, which indicates that there is no change of the mechanism of inhibition in the presence and absence of the extract (Figure 5).

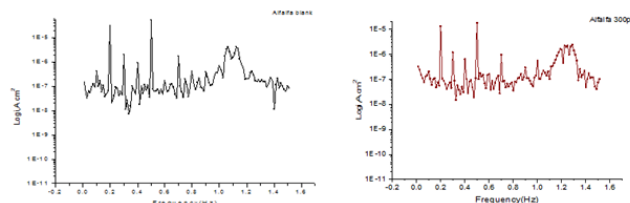


**Figure 9** EFM spectra for CS in polluted NaCl without and with 300ppm of CTE.

### Electrochemical impedance spectroscopy (EIS) measurements

EIS is well-established and it is a powerful technique for studying the corrosion. Surface properties, electrode kinetics and mechanistic information can be obtained from impedance diagrams<sup>26</sup> (Figure 6). Figure 7 shows the Nyquist plots obtained at open circuit potential both in the absence and presence of increasing doses of investigated CTE at 25°C. The increase in the size of the capacitive loop with the addition of investigated extract shows that a barrier gradually forms on the CS surface. The Nyquist plots do not yield perfect semicircles as expected from the theory of EIS. The deviation from ideal semicircle was generally attributed to the frequency dispersion<sup>27</sup> as well as to the inhomogeneities of the surface.

EIS spectra of the investigated extract were analyzed using the equivalent circuit, Figure 6, which represents a single charge transfer



reaction and fits well with our experimental results. The constant phase element, CPE, is introduced in the circuit instead of a pure double layer capacitor to give a more accurate fit.<sup>28</sup> The double layer capacitance,  $C_{dl}$ , for a circuit including a CPE parameter ( $Y_0$  and  $n$ ) were calculated the following Eq. 10:<sup>29</sup>

$$C_{dl} = Y_0 \omega n - 1 / \sin[n(\pi / 2)] \quad (10)$$

Where  $Y_0$  is the magnitude of the CPE,  $\omega = 2\pi f_{max}$ ,  $f_{max}$  is the frequency at which the imaginary component of the impedance is maximal and the factor  $n$  is an adjustable parameter that usually lies between 0.5 and 1.0. After analyzing the shape of the Nyquist plots, it is concluded that the curves approximated by a single capacitive semicircles, showing that the corrosion process was mainly charged-

transfer controlled.<sup>30</sup> The general shape of the curves is very similar for all samples (in presence or absence of extract) indicating that no change in the corrosion mechanism.<sup>31</sup> From the impedance data (Table 6), we concluded that the value of  $R_{ct}$  increases with increasing the dose of the extract and this indicates an increase in  $\% IE_{EIS}$ , which in concord with the PP results obtained. In fact the presence of extract enhances the value of  $R_{ct}$  in acidic solution. Values of double layer capacitance are also brought down to the maximum extent in the presence of extract and the decrease in the values of CPE follows the order similar to that obtained for  $i_{corr}$  in this study. The decrease in  $CPE/C_{dl}$  results from a decrease in local dielectric constant and/or an increase in the thickness of the double layer, suggesting that organic derivatives inhibit the iron corrosion by adsorption at metal/acid<sup>32</sup> (Figure 8).

**Table 1** Values of  $\% IE$ ,  $\theta$  and corrosion rate (CR) of different doses of Cascabela Thevetia extract for the corrosion of CS from WL measurements at 25°C

Conc., ppm	CR, $\times 10^{-4} \text{ mg cm}^2 \text{ min}^{-1}$	$\theta$	$\% IE$
blank	80	---	---
50	50	0.378	37.8
100	48	0.405	40.5
150	46	0.432	43.2
200	39	0.514	51.4
250	33	0.595	59.5
300	24	0.703	70.3

**Table 2** Data of WL measurements for CS in polluted NaCl solution with and without different doses of CTE at 25-45°C

Conc., ppm	Temp., °C	CR, $\times 10^{-4} \text{ mg cm}^2 \text{ min}^{-1}$	$\theta$	$\% IE$
Blank (3.5% NaCl+ 16 ppmNa <sub>2</sub> S)	25	80	----	----
	30	85	----	----
	35	90	----	----
	40	105	-----	-----
	45	110	-----	-----
50	25	50	0.378	37.8
	30	58	0.306	30.6
	35	67	0.253	25.3
	40	83	0.227	22.7
	45	88	0.217	21.7
100	25	48	0.405	40.5
	30	53	0.361	36.1
	35	60	0.331	33.1
	40	73	0.318	31.8
	45	78	0.304	30.4
150	25	46	0.432	43.2
	30	51	0.389	38.9
	35	58	0.356	35.6
	40	71	0.341	34.1
	45	76	0.326	32.6
200	25	39	0.514	51.4
	30	44	0.472	47.2
	35	51	0.434	43.4
	40	63	0.409	40.9
	45	68	0.391	39.1
250	25	33	0.595	59.5
	30	37	0.556	55.6
	35	44	0.511	51.1
	40	56	0.477	47.7
	45	61	0.457	45.7
300	25	24	0.703	70.3
	30	30	0.639	63.9
	35	35	0.614	61.4
	40	44	0.590	59.0
	45	47	0.585	58.5

**Table 3** Thermodynamic parameters from Freundlich isotherm model for CS in polluted NaCl for investigated extract at different temperatures

Temp. K	$K_{ads} M^{-1}$	$-\Delta G^{\circ}_{ads} kJ mol^{-1}$	$-\Delta H^{\circ}_{ads} kJ mol^{-1}$	$-\Delta S^{\circ}_{ads} J mol^{-1} K^{-1}$
298	0.094	4.1		142.2
303	0.059	3.0		143.5
308	0.038	2.0	46.5	144.6
313	0.032	1.5		143.7
318	0.029	1.3		142.2

**Table 4** Thermodynamic activation parameters for the dissolution of CS in polluted NaCl with and without different doses of investigated extract

Comp	Conc., ppm	$E_a^*, kJ mol^{-1}$	$\Delta H^*, kJ mol^{-1}$	$-\Delta S^*, J mol^{-1} K^{-1}$
Polluted NaCl	0.0	7.0	5.4	263.1
	50	19.1	16.7	232.7
	100	19.3	16.9	232.3
Cascabela thevetia	150	19.9	17.5	231.0
	200	22.0	19.6	225.1
	250	24.9	22.5	217.1

**Table 5**  $E_{corr}$ ,  $i_{corr}$ ,  $\beta_c$ ,  $\beta_a$ ,  $\theta$ , and % IE of CS in polluted NaCl at 25°C for CTE

Conc., ppm	$-E_{corr}, mV$ vs SCE	$i_{corr}, \mu A cm^{-2}$	$\beta_a, mV dec^{-1}$	$\beta_c, mV dec^{-1}$	$k_{corr}, mmy^{-1}$	$\theta$	%IE
Polluted NaCl	980	134.0	95	100	171	--	--
50	971	23.6	98	81	92	0.823	82.3
100	978	22.0	103	72	71	0.835	83.5
150	991	16.1	106	90	67	0.879	87.0
200	969	15.7	89	85	60	0.882	88.2
250	988	9.6	95	79	58	0.928	92.8
300	982	7.4	100	99	57	0.944	94.4

**Table 6** Electrochemical kinetic parameters obtained from EIS technique for CS in polluted NaCl with and without different doses of investigated extract

Conc., ppm	$R_{ct}, \Omega cm^2$	$C_{dl}, F cm^{-2}$	$\theta$	%IE
Polluted NaCl	57	685	-----	-----
50	95	665	0.393	39.3
100	229	550	0.747	74.7
150	258	522	0.779	77.9
200	300	422	0.810	81.0
250	434	230	0.866	86.6
300	650	205	0.912	91.2

### Electrochemical frequency modulation (EFM) measurements

Figure 9 shows the EFM intermodulation spectra (current vs. frequency) of CS in polluted NaCl solutions containing different concentrations of Cascabela Thevetia extract. The larger peaks were used to calculate the corrosion current density ( $i_{corr}$ ), the Tafel slopes ( $\beta_c$  and  $\beta_a$ ) and the causality factors CF-2 and CF-3. These electrochemical parameters were listed in Table 7. The data presented obviously show that, the addition of the tested extract at a given dose to the acidic solution decreases the corrosion current density, indicating that this extract inhibits the corrosion of CS in polluted NaCl through adsorption. The causality factors obtained under different experimental conditions are approximately equal to the theoretical values (2 and 3) indicating that the measured data are verified and of good quality. The inhibition efficiencies % IEEFM increase by increasing the extract doses and was calculated from the following Eq 11.

$$\%IE_{EFM} = \left[ 1 - \left( i_{corr} / i_{corr}^0 \right) \right] \times 100 \quad (11)$$

### Atomic force microscope (AFM) studies

AFM is a new technique to study the influence of extract on the generation and the progress of corrosion at the metal surface. The main advantage of this method is that the roughness of the surface can be

determined. Figure 6(a) showed AFM image of CS specimen before immersion in polluted NaCl in 3D. Figure 6(b) is an image obtained for CS specimen after immersion in polluted NaCl without extracts in 3D. Figure 6(c) referred to CS specimen after 24h in immersion of polluted NaCl + 300 ppm of Cascabela Thevetia extract in 3D.

As shown in Table 8, the lower value of roughness in the presence of extract as compared to its absence that the adsorption of extract molecules on the CS surface. So, it inhibits the corrosion of CS in polluted NaCl, suggested that the extract acts as good corrosion inhibitor. The lower value of roughness in the presence of Cascabela Thevetia suggested that Cascabela Thevetia protects the CS surface in polluted NaCl.

### Mechanism of corrosion inhibition

Cascabela Thevetia extract used as an inhibitor leads to changes in the Tafel slopes, decrease of the corrosion current density, an increase in the charge transfer resistance and decrease in the double layer capacitance through the interference in cathodic and anodic reactions. The mechanism of inhibition is due to the physical adsorption of extract molecules on the CS surface. Most of the Cascabela Thevetia constituents are proteins, lipids, soluble sugar, starch and ash. These molecules may inhibits the corrosion due to:

- a. Formation of complex compounds via chelating with  $\text{Fe}^{2+}$  cations which adsorbed on CS surface, thus prohibiting the adsorption aggressive ions such as  $\text{Cl}^-$  or
- b. The adsorption of the extract molecules on the CS surface due to the donor-acceptor interaction between  $\pi$  electrons of donor atoms of aromatic rings of the molecules and the vacant d orbital of iron surface atoms and/or
- c. The extract molecules can also be adsorbed on the metal surface in the form of negatively charged species which can interact electrostatically with positively charged species metal surface, which led to increase the surface coverage and to increase the IE. Cascabela Thevetia extract provide greater IE due to the large degree of surface coverage resulting from the adsorption of particular molecules or a group of constituents from the crude extract.<sup>34</sup>

## Conclusion

From the results of the study the following may be concluded:

The investigated extract is good corrosion inhibitor for CS in polluted NaCl solution. Results obtained from potentiodynamic polarization indicated that the investigated extract is mixed-type inhibitor. % IE of Cascabela Thevetia extract was temperature dependent and its addition led to an increase of the activation energy. The results of EIS revealed that an increase in the charge transfer resistance and a decrease in double layer capacitance when the extract is added and hence an increase in % IE. This is attributed to increase of the thickness of the electrical double layer. The adsorption of Cascabela Thevetia extract onto CS surface follows the Freundlich adsorption isotherm model (physisorption). Reasonably good agreement was observed between the values obtained by the weight loss and electrochemical measurements.

## Acknowledgments

None.

## Conflicts of interest

None.

## References

1. Quraishi MA, Singh A, Kumar Singh V, et al. Green Approach to Corrosion Inhibition of Mild Steel in Hydrochloric Acid and Sulphuric Acid Solutions by the Extract of *Murraya koenigii* Leaves. *Materials Chemistry and Physics*. 2010;122(1):114–122.
2. Behpour M, Ghoreishi SM, Khayat Kashani M, et al. Approach to Corrosion Inhibition of Mild Steel in Two Acidic Solutions by the Extract of *Punica granatum* Peel and Main Constituents. *Materials Chemistry and Physics*. 2012;131(2):621–633.
3. Abiola OK, James AO. The Effects of *Aloe vera* Extract on Corrosion and Kinetics of Corrosion Process of Zinc in HCl Solution. *Corrosion Science*. 2010;52(2):661–664.
4. El-Etre AY. Khillah extract as inhibitor for acid corrosion of SX 316 steel. *Applied Surface Science*. 2003;252(24):8521–8525.
5. Torres V, Amado R, de Sa C, et al. Inhibitory action of aqueous coffee ground extracts on the corrosion of carbon steel in HCl solution. *Corrosion Science*. 2011;53(7):2385–2392.
6. Majeed M, Sultan A, Al-Sahlanee H. Effect of *Lavandula stoechas* oil on welded material corrosion in 5.5M  $\text{H}_3\text{PO}_4$  solution. *Journal of Chemical and Pharmaceutical Research*. 2013;5(12):1297–1306.
7. Sharmila A, Angelin A, Aarockia Sahayaraj P. Influence of murrayakoenigii (curry leaves) extract on the corrosion inhibition of carbon steel in HCl solution Rasayan. *J Chem*. 2010;3(1):74–81.
8. Odewunmi N, Umoren S, Gasem Z. Utilization of watermelon rind extract as a green corrosion inhibitor for mild steel in acidic media. *Journal of Industrial and Engineering Chemistry*. 2015;21:239–247.
9. Lebrini M, Robert F, Lecante A, et al. Corrosion inhibition of C38 steel in 1 M hydrochloric acid medium by alkaloids extract from *Oxandra asbeckii* plant. *Corrosion Science*. 2011;53(2):687–695.
10. Roy P, Karfa P, Adhikari U, et al. Corrosion inhibition of mild steel in acidic medium by polyacrylamide grafted Guar gum with various grafting percentage: Effect of intramolecular synergism. *Corrosion Science*. 2014;88:246–253.
11. Li L, Zhang X, Lei J, et al. Adsorption and corrosion inhibition of *Osmanthus fragran* leaves extract on carbon steel. *Corrosion Science*. 2012;63:82–90.
12. Fouda AS, Etaiw S, Elnggar W. Punica Plant extract as Green Corrosion inhibitor for C-steel in Hydrochloric Acid Solutions. *International Journal of Innovative Research in Science, Engineering and Technology*. 2014;9:4866–4883.
13. Zarrok H, Zarrouk A, Salghi R, et al. Inhibitive properties and thermodynamic characterization of quinoxaline derivative on carbon steel corrosion in acidic medium. *Der Pharmacia Lettre*. 2013;5:43–53.
14. Fouda AS, Abousalem AS, El-Ewady GY. Mitigation of corrosion of carbon steel in acidic solutions using an aqueous extract of *Titia Cordata* as green corrosion inhibitor. *International Journal of Industrial Chemistry*. 2017;8(1):61–73.
15. Fouda AS, El-Khteb AY, Fakih M. Methanolic extract of Curcumn as green corrosion inhibitor for steel in NaCl polluted solutions. *Indian J Sci Res*. 2013;4(2):219–227.
16. Fouda AS, Abd El-Maksoud SA, Fayed HM. Delonix Regia Leaf extract as environmental friendly and safe corrosion inhibitor for carbon steel in aqueous solutions. *Journal of Electrochemistry and Plating Technology*. 2017.
17. Sliwka-Kaszynska M, Kot-Wasik A, Namiesnik J. Preservation and Storage of Water Samples. *Journal of Critical Reviews in Environmental Science and Technology*. 2003;31(1):33–44.
18. Elewady GY. Pyrimidine Derivatives as Corrosion Inhibitors for Carbon-Steel in 2M Hydrochloric Acid Solution. *Int J Electrochem Sci*. 2008;3:1149–1161.
19. Zaafarany I, Abdallah M. Ethoxylated Fatty Amide as Corrosion Inhibitors for Carbon Steel in Hydrochloric Acid Solution. *Int J Electrochem Sci*. 2010;5(1):18–28.
20. Yurt A, Balaban A, Kandemir SU, et al. Investigation on some Schiff bases as HCl corrosion inhibitors for carbon steel. *Material Chemistry and Physics*. 2004;85(2-3):420–426.
21. Ali SA, Al-Muallema HA, Rahman SU, et al. Bis-isoxazolidines: A new class of corrosion inhibitors of mild steel in acidic media. *Corrosion Science*. 2008;50(11):3070–3077.
22. Ashassi-Sorkhabi H, Es'haghi M. Corrosion inhibition of mild steel in hydrochloric acid by betanin as a green inhibitor. *Journal of Solid State Electrochemistry*. 2009;13(8):1297–1301.
23. Khaled KF. Evaluation of electrochemical frequency modulation as a new technique for monitoring corrosion and corrosion inhibition of carbon steel in perchloric acid using hydrazine carbodithioic acid derivatives. *Journal of Applied Electrochemistry*. 2009;39(3):429–438.
24. Bosch RW, Hubrecht J, Bogaerts WF, et al. Electrochemical Frequency Modulation: A New Electrochemical Technique for Online Corrosion Monitoring. *Corrosion*. 2001;57(1):60–70.

25. Abdel-Rehim SS, Khaled KF, Abd-Elshafi NS. Electrochemical frequency modulation as a new technique for monitoring corrosion inhibition of iron in acid media by new thiourea derivative. *Electrochimica Acta*. 2006;51(16):3269–3277.
26. Yurt A, Bereket G, Kivrak A, et al. Effect of Schiff Bases Containing Pyridyl Group as Corrosion Inhibitors for Low Carbon Steel in 0.1 M HCl. *Journal of Applied Electrochemistry*. 2005;35(10):1025–1032.
27. Macdonald JR, Johanson WB. *Theory in Impedance Spectroscopy*. In: Macdonald JR (Eds.), John Wiley & Sons, New York, USA. 1987.
28. Ivanov ES. *Inhibitors for Metal Corrosion in Acid Media*. Metallurgy, Moscow, Russia. 1986.
29. Bentiss F, Lebrini M, Lagrenee M. Thermodynamic characterization of metal dissolution and inhibitor adsorption processes in mild steel/2,5-bis(n-thienyl)-1,3,4-thiadiazoles/hydrochloric acid system. *Corrosion Science*. 2005;47(12):2915–2931.
30. Lebrini M, Bentiss F, Vezin H, et al. The inhibition of mild steel corrosion in acidic solutions by 2,5-bis(4-pyridyl)-1,3,4-thiadiazole: Structure-activity correlation. *Corrosion Science*. 2006;48(5):1279–1291.
31. Lagrenee M, Mernari B, Bouanis M, et al. Study of the mechanism and inhibiting efficiency of 3,5-bis(4-methylthiophenyl)-4H-1,2,4-triazole on mild steel corrosion in acidic media. *Corrosion Science*. 2002;44(3):573–588.
32. Schmid GM, Huang HJ. Spectro-electrochemical studies of the inhibition effect of 4, 7-diphenyl -1, 10-phenanthroline on the corrosion of 304 stainless steel. *Corrosion Science*. 1980;20(8-9):1041–1057.
33. Khamis E. The Effect of Temperature on the Acidic Dissolution of Steel in the Presence of Inhibitors. *Corrosion*. 1990;46(6):476–484.
34. Oguzie EE. Corrosion inhibitive effect and adsorption behavior of *Hibiscus sabdariffa* extract on mild steel in acidic media. *Portugaliae Electrochimica Acta*. 2008;26(3):303–314.